

## UV Raman Scattering Analysis of Indented and Machined 6H-SiC and $\beta$ -Si<sub>3</sub>N<sub>4</sub> Surfaces

Jennifer J.H. Walter,<sup>1</sup> Mengning Liang,<sup>1</sup> Xiang-Bai Chen,<sup>3</sup> Jae-il Jang,<sup>4</sup> Leah Bergman,<sup>3</sup> John A. Patten,<sup>2</sup> George M. Pharr,<sup>4,5</sup> and Robert J. Nemanich<sup>1</sup>

<sup>1</sup>*Department of Physics, North Carolina State University, Raleigh, NC 27695-8202*

<sup>2</sup>*Department of Manufacturing Engineering, Western Michigan University, Kalamazoo, MI 49008*

<sup>3</sup>*Department of Physics, University of Idaho, Moscow, ID 83843*

<sup>4</sup>*Department of Materials Science and Engineering, University of Tennessee, Knoxville, TN 37996, and*

<sup>5</sup>*Metal and Ceramic Division, Oak Ridge National Lab, Oak Ridge, TN 37830*

### ABSTRACT

UV Raman scattering is employed as a nondestructive structure sensitive probe to investigate the vibrational properties of the wide bandgap, machined and indented surfaces of 6H-SiC and  $\beta$ -Si<sub>3</sub>N<sub>4</sub>. In these materials, the short absorption depth of UV light allows for accurate probing of the surface, and the transparency to visible light allows for analysis of the bulk material. The study on 6H-SiC (0001) included measurements of indentations, and of machined circular (0001) wafer edges. The indentation analysis indicates the response of the material to localized pressures. Machined 6H-SiC wafer edges and machined  $\beta$ -Si<sub>3</sub>N<sub>4</sub> surfaces indicate a ductile response and ductile material removal for machining at cutting depths on a nm and  $\mu$ m scale. Raman scattering measurements of the ductile surfaces and ductile material removed indicate residual structure changes. The residual surface structures could indicate that a high-pressure phase transformation is the origin of a ductile response on machined brittle materials.

### INTRODUCTION

It has been suggested that the brittle materials,  $\beta$ -Si<sub>3</sub>N<sub>4</sub> and 6H-SiC (0001), can be machined in a ductile regime [1,2]. In this study, the residual structures of the machined surfaces are investigated. These residual structures provide evidence of the origin of the ductile response. During the machining process, high pressures can be achieved at the contact interface between the machining tool and the surface of the material. The high pressures can cause transformation to occur through a series of phases. Upon releasing the pressure, the material can again be transformed to a new phase. Based on prior studies it has been suggested that  $\beta$ -Si<sub>3</sub>N<sub>4</sub> may transform to an unidentified high-pressure phase [1]. Additionally, previous work of 6H-SiC indicates transformation in phase with high pressures [3,4]. A transition from covalent to metallic bonding that is caused from high pressures at the contact interface of the machining tool and the material may produce a ductile surface on machined brittle materials. In the case of point pressures, the non-hydrostatic stress component can influence the transition process. An understanding of the structural transformation process that can occur during machining can lead to improved manufacturing process by establishing parameters that will produce a ductile surface on brittle materials.

### EXPERIMENTAL DETAILS

The 6H-SiC samples used for indentation were supplied by Cree Inc., and the wafers used for machining were purchased from SiCrystal AG. The wafers are circular with a 50 mm diameter

and 250  $\mu\text{m}$  thickness. Both the indented, and machined SiC wafers were transparent to visible light and had a light green color.

The  $\beta\text{-Si}_3\text{N}_4$  sample surfaces were prepared first by grinding and then machining over the ground surface. The machining was employed for depths of cut of 5  $\mu\text{m}$ . The presence of the Si inclusion in the bulk material was deduced from visible Raman spectra, which show a peak at 520  $\text{Rcm}^{-1}$  ( $\text{Rcm}^{-1}$  represents the Stokes shift of the Raman scattering peak).

The indentation experiments were performed on a polished (0001) 6H-SiC surface using a Nanoindenter – XP (MTS, Oak Ridge, TN). This surface corresponds to the Si-face of an ideally terminated structure. A Berkovich diamond indenter tip shaped as a three-sided pyramid with a centerline-to-face angle,  $\Psi$ , of  $65^\circ$  was used to create triangular shaped indentations. The tip was brought into contact with the material at a constant loading rate of 5 mN/sec under a maximum load of 200 mN. The 6H-SiC (0001) machined wafer edges were machined with a sharp tip at rake angles of  $-45^\circ$  and depths of cut of 50 nm. A machining rate of 20 rev./min was employed. Tool wear can change the sharpness of the tip with use, and therefore, alter the pressures that are achieved at the contact interface of the tool and the material. For the limited machining distances in these experiments, tool wear was not expected to significantly influence the machining results, and was therefore, not considered an issue [5].

The Raman scattering experiments were performed with a micro-focus UV spectrometer, and a micro-focus visible spectrometer. In the micro UV Raman system, a  $180^\circ$  backscattering geometry was employed and the laser was focused to a spot size of  $\sim 600$  nm on the sample. The Raman experiments were also performed with the 244 nm line of a frequency doubled Ar ion laser (Lexel Inc.) and the 325 nm line of a HeCd laser (Kimmon Electric), and the scattered light was focused on the entrance slit of a triple spectrometer (Dilor). CCD detection was used to collect the spectra. In the visible macro system, a  $45^\circ$  backscattering geometry was employed, and the laser was focused to a spot size of  $\sim 100$   $\mu\text{m}$  x  $\sim 2$  mm on the sample. The Raman experiments were performed with the 514.5 nm line of an argon ion laser (Coherent Inc.), and the scattered light was focused onto the entrance slit of a double spectrometer (U1000). Photomultiplier detection was used to collect the spectra. The probing depth into crystalline 6H-SiC with a 244 nm incident wavelength is  $\sim 35$  nm and non-crystalline  $\beta\text{-Si}_3\text{N}_4$  is  $\sim 1.4$   $\mu\text{m}$  (the values are calculated for the depth in which the intensity of the light is 37% of the incident intensity) [6].

## RESULTS AND DISCUSSION

Indentation experiments were performed on a 6H-SiC (0001) wafer to investigate the local bonding properties from controlled point pressure conditions. A SEM image of an indented region and the corresponding micro UV Raman measurements are presented in Fig.1. The indentation was performed with a 200 mN maximum load, and the SEM of the indented region indicates an inelastic response with limited macro cracking and some chipping. Micro-focus Raman scattering measurements were obtained from the indent and the surrounding region. Within the indent, the TO (atomic vibrations perpendicular to the  $c$ -axis), and the LO (atomic vibrations parallel to the  $c$ -axis) modes are displaced to higher relative wavenumbers when compared to the reference spectrum, which was obtained far from the indent. The peak displacements indicate compressive stresses. A maximum displacement was observed in the

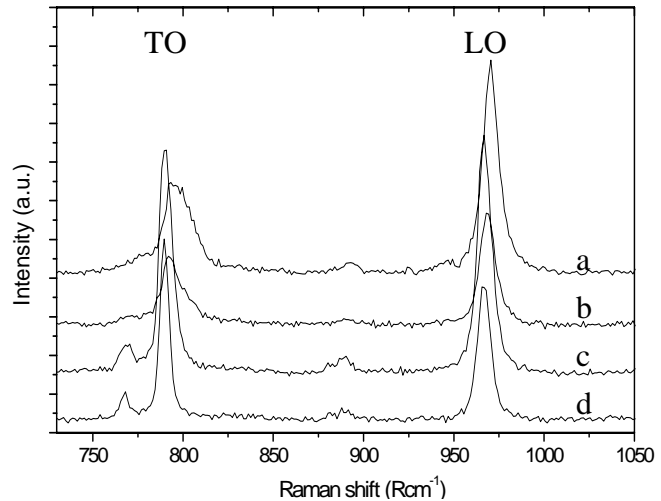
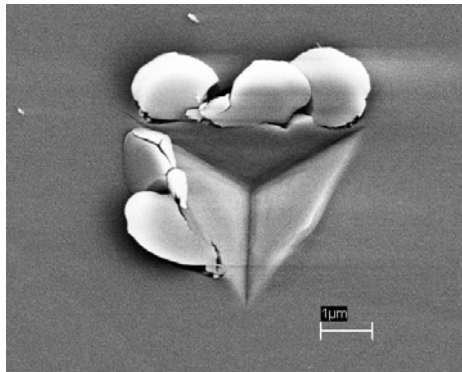


FIG 1: SEM image after indentation with a maximum load of 200 mN. The UV micro Raman scattering spectra display the TO, and LO modes for the (a) center of the indent (b) edge of the indent (c) surrounding area (d) reference area.

center of the indent. The peak displacements signify that the region at the contact point of the diamond tip, and the 6H-SiC is the zone of maximum stress. The stress decreases outward from the center. The center peak position of the TO mode is shifted by a larger amount than the center peak position of the LO mode, this may indicate that the material is under biaxial compression. The Raman scattering spectra do not show evidence of residual structural changes within the indentation. It is possible that a transformed region under the indenter may be very small or may have been extruded as debris. It is notable that the stresses indicate that the surrounding regions have not been completely relaxed with micro cracking.

Optical microscope inspection of the 6H-SiC machined wafer edges also indicates a ductile response from the machining process. The observation of a ductile response was found to be dependent on several parameters of the machining process including tool rake angle, cutting speed, surface orientation, and depth of cut. For a range of cutting depths between 50 and 500 nm, the 50 nm cutting depth produced almost completely ductile surfaces, while the 500 nm cutting depth produced almost completely brittle surfaces for all of the machined surfaces. The material removed during machining indicated elongated, ductile chips, in addition to the fractured and brittle chips. The percentage of ductile chips removed increased with shallower depths of cut, which is probably a direct consequence of the increased ductile surface area with the shallower depth of cut.

Raman scattering measurement of a machined 6H-SiC wafer edge acquired from the  $[11\bar{2}0]$  wafer direction is shown in Fig. 2. Optical inspection of the machined surface indicated a ductile response. A spectrum of crystalline 6H-SiC obtained from a reference wafer edge, and the calculated phonon density of states for SiC is shown for comparison [7]. The spectrum of the machined edge indicates broadened peaks, and the TO mode center frequency is displaced to a higher relative wavenumber while the LO mode center frequency is displaced to a lower relative wavenumber from their crystalline peaks. The broadened displaced TO peak may be attributed to random oriented polycrystalline material since the TO mode frequency will shift with phonon propagation direction [8]. Because of the width of the features, the presence of residual stress

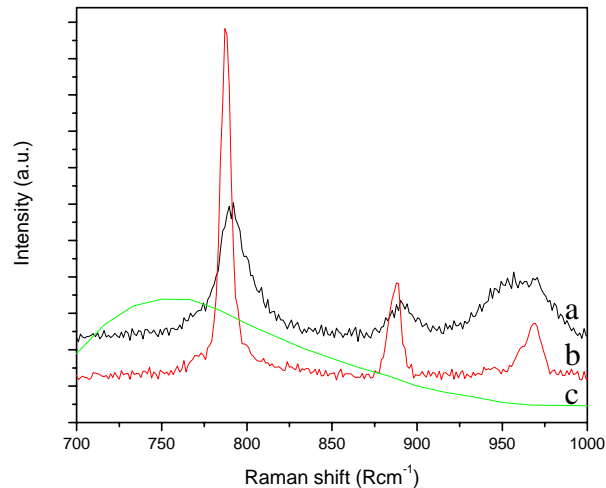


FIG 2: UV micro Raman scattering spectra of (a) machined ductile 6H-SiC edge, and a (b) non-machined 6H-SiC wafer edge. For comparison, the (c) calculated vibrational density of states (DOS) of SiC is presented [7].

cannot be excluded from these measurements. The TO and LO mode splitting is derived from both the anisotropy of the material, and an electrostatic component generated from the charge transfer between the Si and C atoms. A decrease in the TO-LO splitting could indicate small grain size polycrystalline material since the long range electrostatic interaction would be limited by the crystal domain size.

The  $\beta$ -Si<sub>3</sub>N<sub>4</sub> surfaces were machined to further investigate the response of brittle materials to point pressures. It was found that for machining depths on a  $\mu\text{m}$  and nm scale, a smooth, ductile surface could be obtained. Fig. 3 presents the Raman scattering spectra of the machined  $\beta$ -Si<sub>3</sub>N<sub>4</sub> surface for a 5  $\mu\text{m}$  machining depth of cut and incident wavelengths of 514.5, 325, and 244 nm. The 514.5 nm visible Raman scattering spectrum indicates sharp crystalline peaks. The 325 nm incident wavelength indicates slightly broader peaks, but the broad background is enhanced at shorter wavelengths. The spectrum obtained with 244 nm excitation indicates completely broadened features. It has been reported that the broadened density of states of Si<sub>3</sub>N<sub>4</sub> contains two broadened peaks centered at about  $\sim 400$  and  $\sim 900$  Rcm<sup>-1</sup> [9], thus suggesting the presence of amorphous Si<sub>3</sub>N<sub>4</sub> at the machined surface. The depth of the amorphous region can be estimated from comparison between the spectra obtained with different incident wavelengths. The spectrum obtained with 324 nm excitation shows significant amorphous and crystalline signatures suggesting that the amorphous layer thickness is similar to the absorption depth of the light.

Similar to the 6H-SiC, the  $\beta$ -Si<sub>3</sub>N<sub>4</sub> material removed during the machining process also indicates a ductile response. A SEM image of a  $\beta$ -Si<sub>3</sub>N<sub>4</sub> chip removed during the machining process and micro and macro Raman scattering measurements obtained from a large quantity of the chips pressed together are presented in Fig. 4. The SEM image indicates that the chips were bent and distorted without fracture. The broadened peaks indicated in the micro and macro Raman scattering spectra indicate that the chips are amorphous. There is some extent of crystalline

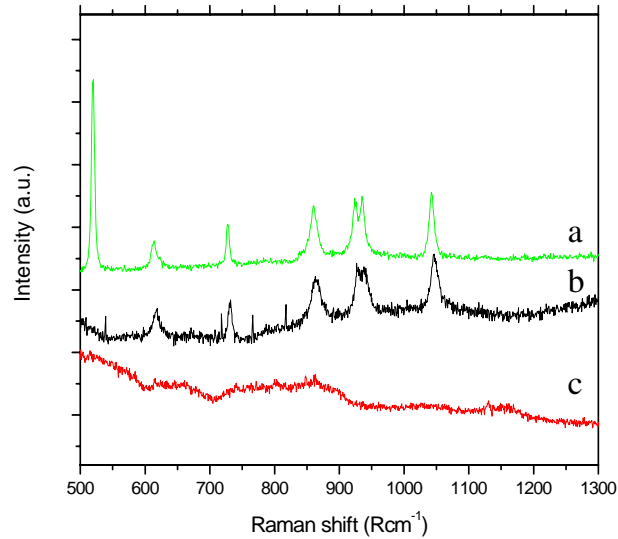
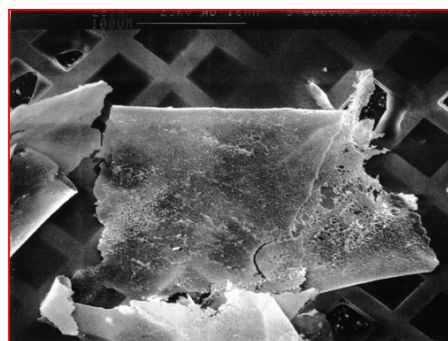


FIG 3: (a) Macro Raman scattering spectrum of machined  $\beta$ - $\text{Si}_3\text{N}_4$  obtained with 514.5 nm excitation, and micro Raman scattering spectra obtained with (b) 325 and (c) 244 nm excitation.

peaks observed in the micro Raman scattering spectrum indicating that the power density produced by the small spot size in micro Raman scattering spectrum was high enough to heat and crystallize the chips.

The residual surface layers on ductile-machined 6H-SiC and  $\beta$ - $\text{Si}_3\text{N}_4$  could be relaxed structures of high-pressure phases that were generated in the local regions due to the point pressures from the indenting and machining processes. Therefore, the residual structures may provide evidence of the origin of the ductile behavior. In our measurements, the transformed regions are observed on machined surfaces that exhibit a ductile response. Furthermore, it is not likely that the polycrystalline surface layer on the machined 6H-SiC wafer edges is a direct transformation from the parent crystalline structure since the transformation would involve randomly orienting



400 x 400 $\mu\text{m}$

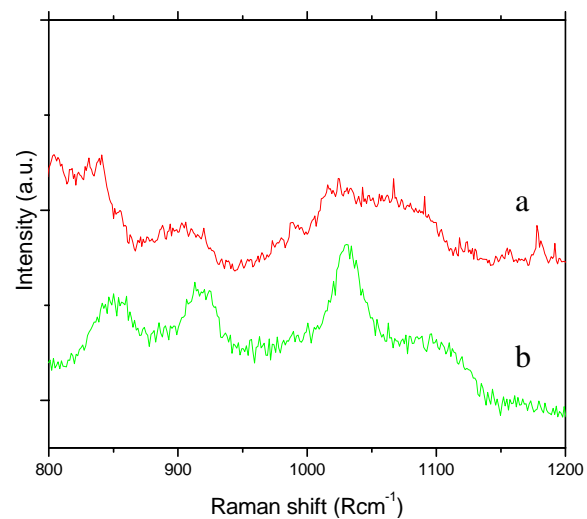


FIG 4: SEM image of a  $\beta$ - $\text{Si}_3\text{N}_4$  chip, and (a) macro and (b) micro Raman scattering spectra of the chips produced during machining at a 5  $\mu\text{m}$  depth of cut.

the crystal. A polycrystalline phase could, however, result from recrystallization during a nucleation and growth process that occurs during relaxation from the high-pressure phase. In  $\beta$ - $\text{Si}_3\text{N}_4$ , the residual amorphous phase may be a direct result of the high-pressure process or it could result from relaxation of a high-pressure phase. A transition to a metallic high-pressure phase has been considered for point pressure processes on Si, and it is possible that the same effect could account for the observations on both 6H-SiC and  $\beta$ - $\text{Si}_3\text{N}_4$  surfaces.

## CONCLUSIONS

It has been found that the surfaces of the brittle materials, 6H-SiC and  $\beta$ - $\text{Si}_3\text{N}_4$ , can be precision engineered in a ductile regime. The indentation experiments indicate that point pressures on 6H-SiC (0001) produce a compressive biaxial stress in the local bonding structure. In the indentations, if transformation has occurred, the region of transformed material may be too small to detect a residual structure change. Machining of 6H-SiC (0001) wafer edges also indicates ductile response. UV Raman scattering measurements suggest that the ductile surfaces have a polycrystalline surface layer. Furthermore, it has also been found that  $\beta$ - $\text{Si}_3\text{N}_4$  can be machined in a ductile regime. The ductile surfaces indicated an amorphous surface layer. The material removed during machining also indicates a ductile response, and an amorphous phase. We have suggested that the transformation to a polycrystalline phase on the 6H-SiC wafer edges occurs through the nucleation of growth of the crystalline phase. Therefore, these structural transformations are suggestive that a high-pressure phase transformation to a metallic phase during the machining process is the origin of the ductile response of the machined surfaces of these brittle materials.

## ACKNOWLEDGEMENTS

The research was sponsored by The National Science Foundation under grant numbers FRG 0203552 and DMR 0403650.

## REFERENCES

1. J. Patten, R. Fesperman, S. Kumar, S. McSpadden, J. Qu, M. Lance, J. Huening, R. Nemanich, *Appl. Phys. Lett.* **83**, 4740 (2003).
2. L. Yin, E. Y. J. Vancoille, K. Ramesh, H. Huang, *Int. J. Manuf. Tool Manu.* **44**, 607 (2004).
3. M. Yoshida, A. Onodera, M. Ueno, K. Tekemura, and O. Shimomura, *Phys. Rev. B* **48**, 10587 (1993).
4. T. Sekine and T. Kobayashi, *Phys. Rev. B* **55**, 8034 (1997).
5. J. Patten, W. Gao, K. Yasuto, accepted for publication *J. Manuf. Sci. E.-T. ASME* (2004).
6. "Handbook of optical constants", E.D. Palik, ed. (Academic, Orlando, Fla. 1985).
7. A. Chehaidar, R. Carles, A. Zwick, C. Meunier, B. Cros, J. Durand, *J. Non-Crys. Solids* **169**, 37 (1994).
8. D.W. Feldman, J.H. Parker, JR., W.J. Choyke, Lyle Patrick, *Phys. Rev.* **173**, 787 (1968).
9. N. Wafa, S.A. Solin, J. Wong, and S. Prochazka, *J. Non-Crys. Solids* **43**, 7 (1981).